

# Exotic Lifshitz transitions in topological materials

G.E. Volovik<sup>1,2,3</sup>

<sup>1</sup>*Low Temperature Laboratory, Aalto University, P.O. Box 15100, FI-00076 AALTO, Finland*

<sup>2</sup>*L. D. Landau Institute for Theoretical Physics, 117940 Moscow, Russia*

<sup>3</sup>*P.N. Lebedev Physical Institute, RAS, Moscow 119991, Russia*

(Dated: October 31, 2022)

Topological Lifshitz transitions involve many types of topological structures in momentum and frequency-momentum spaces: Fermi surfaces, Dirac lines, Dirac and Weyl points, etc. Each of these structures has their own topological invariant ( $N_1, N_2, N_3, \tilde{N}_3$ , etc.), which supports the stability of a given topological structure. The topology of the shape of Fermi surfaces and Dirac lines, as well as the interconnection of the objects of different dimensions, lead to numerous classes of Lifshitz transitions. The consequences of Lifshitz transitions are important in different areas of physics. The singularities emerging at the transition may enhance the transition temperature to superconductivity; the Lifshitz transition can be in the origin of the small masses of elementary particles in our Universe; the black hole horizon serves as the surface of Lifshitz transition between the vacua with type-I and type-II Weyl points; etc.

PACS numbers:

## I. INTRODUCTION. FERMI SURFACE, DIRAC LINE, WEYL POINT

The key word in consideration of Lifshitz transitions is topology. Following original Lifshitz paper,<sup>1</sup> Lifshitz transition has been viewed as a change of the topology of the Fermi surface without symmetry breaking. Later it became clear that topology of the shape is not the only topological characterization of the Fermi surface. Fermi surface itself represents the singularity in the Green's function, which is topologically protected: it is the vortex line in the four-dimensional frequency-momentum space in Fig. 1 (*top right*). The stability of the Fermi surface under interaction between the fermions is in the origin of the Fermi liquid theory developed by Landau. Moreover, the Fermi surface appeared to be one in the series of the topologically stable singularities,<sup>2,3</sup> which include in particular the Weyl point – the hedgehog in momentum space in Fig. 1 (*middle*) and the Dirac line – the vortex line in the three-dimensional momentum space in Fig. 1 (*bottom*). The stability of these objects is supported by the corresponding topological invariants in momentum space or in extended frequency-momentum space.

The combination of topology of the shape of the Fermi surfaces, Fermi lines and Fermi points together with the topology, which supports the stability of these objects, and also the topology of the interconnections of the objects of different dimensions provide a large number of different types of Lifshitz transitions (some of the are discussed in Refs.<sup>4,5</sup>). This makes the Lifshitz transitions ubiquitous with applications to high energy physics, cosmology, black hole physics and to search for the room- $T$  superconductivity.

In particular, the Lifshitz transition may give the solution of the hierarchy problem in particle physics: why the masses of elementary particles in our Universe are so extremely small compared with the characteristic Planck energy scale. Indeed, when we compare the mass  $\sim 10^2$

GeV of the most heavy particle – the top quark – with the Planck energy  $\sim 10^{19}$  GeV, we can see that the vacuum of our Universe is practically gapless. There are several topological scenarios, which may lead to the (almost) gapless vacuum. In one scenario the vacuum belongs to the class of Weyl materials, where the nodes in the spectrum of elementary particles – the Weyl points – are topologically protected,<sup>2,3,8</sup> see Sec.III and Fig. 4. According to this scenario the physical laws are not fundamental, but emerge in the low energy corner of the quantum vacuum, i.e. in the vicinity of the Weyl points, where all the symmetries emerge from nothing. At even lower energy some of these symmetries experience spontaneous breaking, analogous to the superconducting transition. In the latter case the hierarchy problem is understood: in most superconductors the transition temperature  $T_c$  is exponentially small, compared to the characteristic Fermi energy scale (analog of Planck scale), and we are searching for the exceptional materials with enhanced  $T_c$ .

In the other scenario, the massless (gapless) vacua emerge at the Lifshitz transition between the fully gapped vacua with different topological charges, see Sec.VII and Fig. 12. The almost perfect masslessness of elementary particles in our Universe suggests that the Universe is very close to the line of the topological Lifshitz transition, at which fermions necessarily become gapless.<sup>9</sup> This is the topological analog of the so-called Multiple Point Principle, according to which the Universe lives at the coexistence point (line, surface, etc.) of the first order phase transition, where different vacua have the same energy.<sup>10–14</sup>

The application of the Lifshitz transition to the black hole physics will be considered in Sec. VI, while the role of the Lifshitz transition in the enhancement of the temperature of superconducting transition is in Sec. VIII.

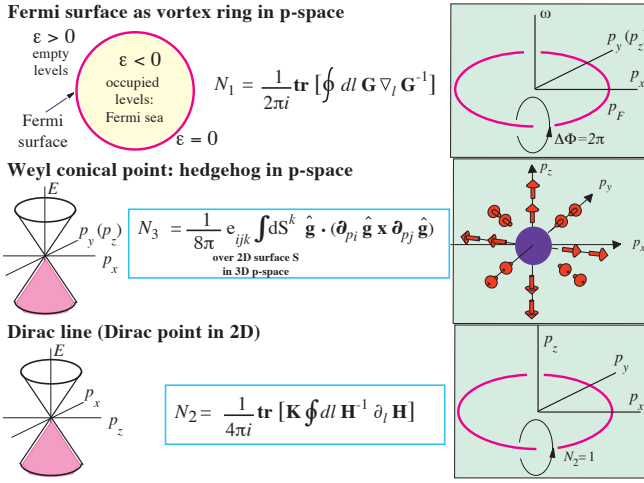


FIG. 1: Topologically stable nodes in the energy spectrum of electrons in metals or fermions in general.

(*Top*): Fermi surface represents the singularity in the Green's function, which forms the vortex in the 3 + 1 ( $\mathbf{p}, \omega$ )-space, see Sec. II and Fig. 2 (in the 2 + 1 ( $p_x, p_y, \omega$ )-space this is the vortex line). The stability of the vortex is supported by the winding number – the integer-valued invariant  $N_1$ , expressed in terms of the Green's function.

(*Middle*): Conical point in the fermionic spectrum of the Weyl materials (Weyl semimetals, chiral superfluid  $^3\text{He-A}$ , and the vacuum of Standard Model in its gapless phase, see Sec. III and Fig. 4). The directions of spin (or of the emergent spin, isospin, pseudo-spin, etc.) form the topological object in momentum space – the hedgehog or the Berry phase monopole<sup>6</sup> – described by the integer-valued topological invariant  $N_3$ .

(*Bottom*): Dirac lines – lines of zeroes in the energy spectrum, described by the topological invariant  $N_2$ . The circular line is the Dirac line in the quasiparticle spectrum in the polar phase of superfluid  $^3\text{He}$ , which has been recently created in aerogel.<sup>7</sup> The same invariant  $N_2$  stabilizes the point nodes in 2D materials, such as graphene.

## II. FERMI SURFACE AS TOPOLOGICAL OBJECT

The primary topology, which is at the origin of the Lifshitz transitions, is the topology which is responsible for the stability of the Fermi surface. If the Fermi surface is not stable under the electron-electron interaction, the consideration of the topology of the shape of the Fermi surface and of the corresponding Lifshitz transitions does not make much sense. To view the topological stability of the Fermi surface with respect to interactions let us start with the Green's function of an ideal Fermi gas in Fig. 2 (*left*). The Fermi surface  $\epsilon(\mathbf{p}) = 0$  of the non-interacting Fermi gas is the boundary in momentum space, which separates the occupied states with  $\epsilon(\mathbf{p}) < 0$  from the empty states with  $\epsilon(\mathbf{p}) > 0$ . The Green's function  $G(\omega, \mathbf{p})$  with  $\omega$  on imaginary axis

$$G^{-1}(\omega, \mathbf{p}) = i\omega - \epsilon(\mathbf{p}), \quad (1)$$

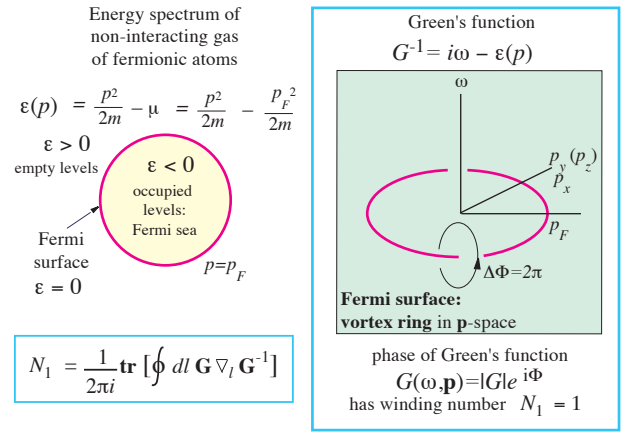


FIG. 2: Fermi surface is robust to interactions because it represents the topologically stable singularity in the Green's function – the vortex the 3 + 1 ( $\mathbf{p}, \omega$ )-space. The stability of the vortex is supported by the winding number of the phase  $\Phi$  of the Green's function  $G = |G|e^{i\Phi}$ . In general the winding number is given by the integer-valued invariant  $N_1$ , expressed in terms of the Green's function.

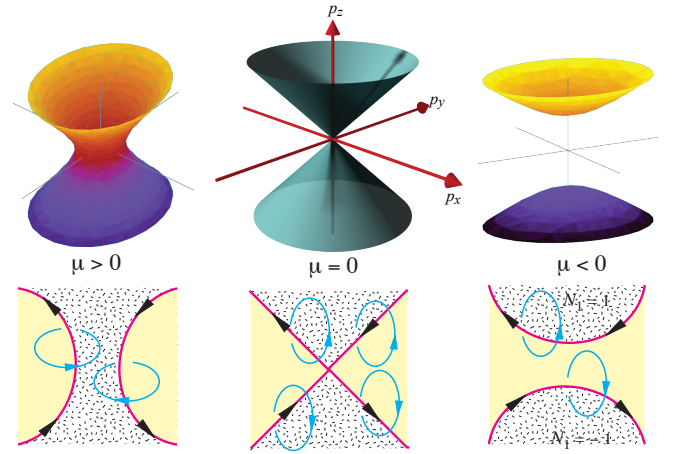


FIG. 3: Since the Fermi surface represents the vortex in the 3+1 ( $\mathbf{p}, \omega$ ) space, the Lifshitz transition with disruption of the neck of the Fermi surface<sup>1</sup> (*top*) is equivalent to the interconnection of vortices (*bottom*).

has singularity at  $\omega = 0$  and  $\epsilon(\mathbf{p}) = 0$ . In Fig. 2 (*right*) the  $p_z$  coordinate is suppressed, and the Green's function singularity forms the closed line in the 2 + 1 momentum-frequency space ( $p_x, p_y, \omega$ ). This line represents the vortex line, at which the phase of the Green's function  $\Phi(p_x, p_y, \omega)$  has the  $2\pi$  winding. As in the case of the real-space vortex in superfluids, the integer winding number provides the stability of the Fermi surface with respect to perturbations, including the interaction (if the  $p_z$  component is restored, the singularity forms the vortex sheet in the 3 + 1 momentum-frequency ( $\mathbf{p}, \omega$ ) space).

In general case, when the Green's function has the spin,

band and other indices, the winding number can be written as the following topological invariant in terms of the Green's function:

$$N_1 = \text{tr} \oint_C \frac{dl}{2\pi i} G(\omega, \mathbf{p}) \partial_l G^{-1}(\omega, \mathbf{p}). \quad (2)$$

Here the integral is taken over an arbitrary contour  $C$  around the momentum-frequency vortex sheet, and  $\text{tr}$  is the trace over all the indices.

Due to topological stability one cannot make a hole in the Fermi surface. As in the case of vortex lines, which cannot terminate in bulk, the Fermi surface has no edges. The Lifshitz transitions take place when the Fermi surface crosses the stationary point of the electronic spectrum. Near the transition the expansion of the generic spectrum has the form:<sup>1</sup>

$$\epsilon_{\mathbf{p}} = ap_x^2 + bp_y^2 + cp_z^2 - \mu. \quad (3)$$

For  $a > 0$ ,  $b > 0$ ,  $c < 0$  the transition with disruption of the neck of the Fermi surface at  $\mu = 0$  is in Fig. 3 (*top*). In terms of the vortex singularities of the Green's function in 3+1  $(\mathbf{p}, \omega)$  space, this Lifshitz transition represents the interconnection of the vortex lines in Fig. 3 (*bottom*). In superfluids, the interconnection of the real-space vortices is an important process in the vortex turbulence.<sup>15</sup>

### III. LIFSHITZ TRANSITIONS GOVERNED BY WEYL POINT TOPOLOGY

Weyl particles are the elementary particles of our Universe. These massless particles are described the  $2 \times 2$  Hamiltonians:  $H = c\boldsymbol{\sigma} \cdot \mathbf{p}$  for right-handed quarks and leptons and  $H = -c\boldsymbol{\sigma} \cdot \mathbf{p}$  for the left-handed particles. Their spins in momentum space form correspondingly the hedgehog and anti-hedgehog in Fig. 4 (*top*). The hedgehog is the topologically stable object, and thus the isolated Weyl points are topologically protected. The corresponding topological invariant for the hedgehogs,  $N_3$ , is also expressed in terms of the Green's function as a surface integral in the 3+1 momentum-frequency space  $p_\mu = (\mathbf{p}, \omega)$ :<sup>3</sup>

$$N_3 = \frac{\epsilon_{\mu\nu\rho\sigma}}{24\pi^2} \text{tr} \oint_{\Sigma_a} dS^\sigma G \frac{\partial}{\partial p_\mu} G^{-1} G \frac{\partial}{\partial p_\nu} G^{-1} G \frac{\partial}{\partial p_\rho} G^{-1}. \quad (4)$$

Here  $\Sigma_a$  is a three-dimensional surface around the isolated Weyl point in  $(\mathbf{p}, \omega)$  space.

From the point of view of the general properties of the fermionic spectrum, the Weyl point represents the exceptional point of level crossing analyzed by von Neumann and Wigner<sup>16</sup>. This analysis demonstrates that two branches of spectrum, which have the same symmetry, may touch each other at the conical (or diabolical) point in the three-dimensional space of parameters. The touching of two branches is described in general

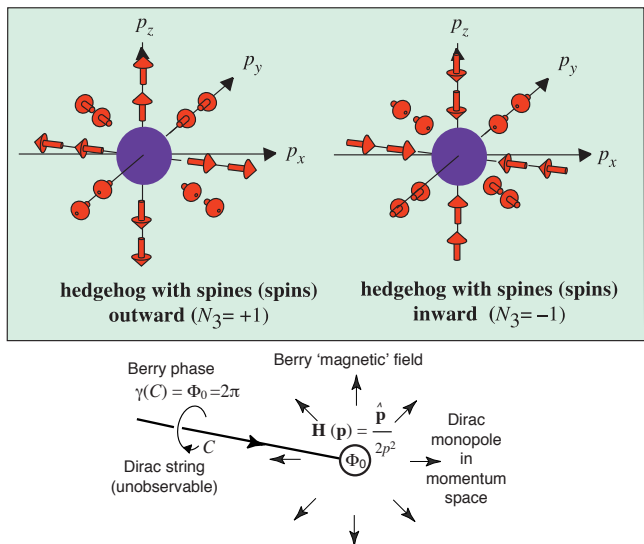


FIG. 4: Spins of the right-handed Weyl particles (quarks and leptons) are directed along the momentum  $\mathbf{p}$  forming the hedgehog (*top left*). The anti-hedgehog – the hedgehog with spines (spins) inward (*top right*) corresponds to the left-handed Weyl particles. The topological invariant  $N_3$  describing the topologically distinct hedgehog configurations is expressed either in terms of the Green's function in Eq.(4) or in terms of the unit vector field in Fig. 1 (*center*).

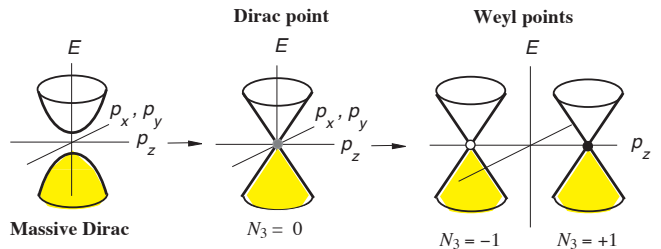


FIG. 5: Formation of the pair of Weyl points from the vacuum state with massive Dirac fermions. Topological charges  $N_3 = +1$  and  $N_3 = -1$  correspond to right-handed and left-handed particles respectively. At the Lifshitz transition the vacuum is gapless with the Dirac point in the fermionic spectrum which has topological charge  $N_3 = 0$ .

by  $2 \times 2$  Hamiltonian  $H = \boldsymbol{\sigma} \cdot \mathbf{g}(\mathbf{p})$ . The topological invariant  $N_3$  is expressed in terms of the unit vector  $\hat{\mathbf{g}}(\mathbf{p}) = \mathbf{g}(\mathbf{p})/|\mathbf{g}(\mathbf{p})|$  in Fig. 1 (*center*), which forms the hedgehog configuration in Fig. 1 (*middle right*). The touching point also represents the Berry phase monopole in Fig. 4 (*bottom*).<sup>6</sup>

The typical Lifshitz transition, which involves the Weyl nodes in the fermionic spectrum, describes the formation of the Weyl points with opposite charges  $N_3 = \pm 1$  from the fully gapped state. Fig. 5 shows the formation of the pair of the Weyl points from the vacuum state with massive Dirac fermions. The intermediate state has the massless Dirac point in the fermionic spectrum with topological charge  $N_3 = 0$ . In electronic systems the in-

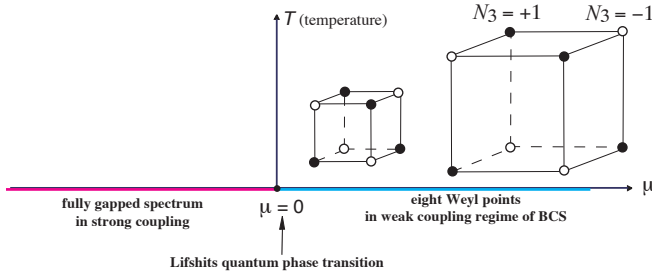


FIG. 6: The same as in Fig. 5, but with formation of 4 right-handed and 4 left-handed Weyl points at vertices of cube. Such arrangement of the Weyl nodes has been discussed for the energy spectrum in superconductors, which belong to the  $O(D_2)$  symmetry class.<sup>17,18</sup> In relativistic theories such arrangement gives 8 left and 8 right Weyl fermions on the vertices of the cube in the 3+1  $(p_x, p_y, p_z, \omega)$  space.<sup>19,20</sup>

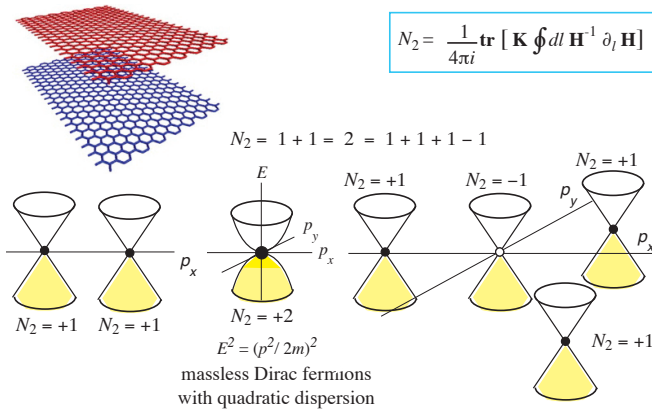


FIG. 7: Lifshitz transition governed by conservation of the topological charge  $N_2$  in bilayer graphene. Two conical points with the same charge  $N_2 = 1$  on two graphene layers merge and form the Dirac point with topological charge  $N_2 = 2$ . The spectrum in the vicinity of such Dirac point is quadratic. This point in turn may split into four Dirac conical points (trigonal warping). The total topological charge is conserved:  $N_2 = 1 + 1 + 1 - 1 = 2$ .

intermediate gapless states can be more complicated with different dispersion relation along different axes (say, linear and quadratic).

Fig. 6 demonstrates the formation of 4 right-handed and 4 left-handed Weyl points. Such arrangement of the Weyl nodes is typical for the energy spectrum in the  $O(D_2)$  symmetry class of the pair correlated systems.<sup>17,18</sup> In both cases the total topological charge  $N_3$  (total) = 0, and thus there is an even number of Weyl fermions, which supports the fermion doubling principle.<sup>21</sup>

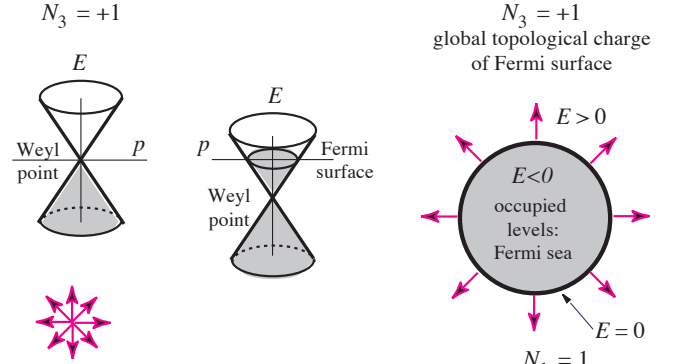


FIG. 8: Fermi surface with local topological charge  $N_1$  and the global topological charge  $N_3$ .

#### IV. LIFSHITZ TRANSITION GOVERNED BY CONSERVATION OF $N_2$ CHARGE

The conservation of the total topological charge in the Lifshitz transitions in Figs. 5 and 6 takes place also in the transitions involving the other topological charges, such as  $N_1$  and  $N_2$ . The topological charge  $N_2$  in Fig. 7 (*top right*) stabilizes the conical Dirac point in graphene and the nodal lines in the 3D semimetals and nodal superconductors.<sup>4</sup> Here  $K$  is the proper symmetry operator, which commutes or anticommutes with the Hamiltonian.

The Lifshitz transition governed by the conservation of the topological charge  $N_2$  is shown in Fig. 7 (*bottom*) on example of bilayer graphene, when one graphene layer is shifted with respect to the other one. Merging of the two conical points with  $N_2 = 1$  leads to formation of the Dirac node with quadratic dispersion, which has the topological charge  $N_2 = 2$ . This point in turn may split into four Dirac conical points with  $N_2 = \pm 1$  (this is the so-called trigonal warping). The total topological charge is conserved,  $N_2 = 1 + 1 + 1 - 1 = 2$ .

#### V. LIFSHITZ TRANSITIONS WITH SEVERAL TOPOLOGICAL CHARGES

In previous sections we considered the Lifshitz transitions, governed by the conservation of a single topological charge: the charge  $N_1$  in Fig. 3;  $N_2$  in Fig. 7; and  $N_3$  in Figs. 5 and 6. However, the objects in momentum space can be characterized simultaneously by several topological invariants. Example of combined topology is in Fig. 8. When the Weyl point shifts from the zero energy position, the Fermi surface is formed. As for all other Fermi surfaces, its stability is supported by the topological invariant  $N_1$ . But in addition the Fermi surface contains the  $N_3$  charge, which can be obtained from Eq.(4) by integration over the surface, which encloses the Fermi

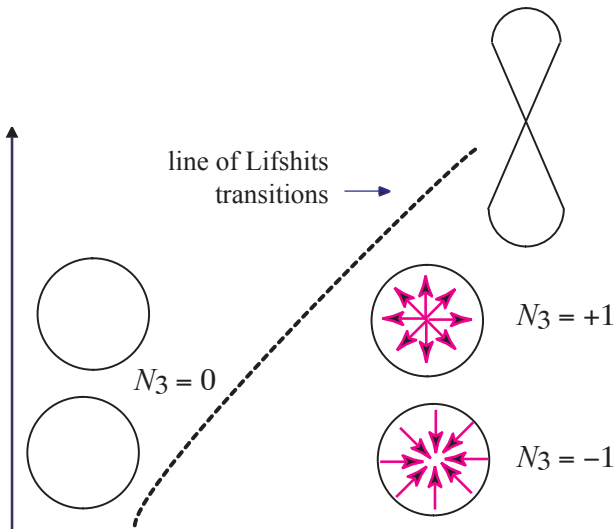


FIG. 9: Lifshitz transition, at which the Fermi surfaces lose the Weyl charge  $N_3$ .<sup>22</sup> The states on both sides of the transition have Fermi surfaces. On the right side of transition the Fermi surfaces contain Weyl points with nonzero topological charges  $N_3 = +1$  and  $N_3 = -1$ . At the transition line, the Fermi surfaces touch each other, and their topological global charges annihilate each other. On the left side of transition the Fermi surfaces are topologically trivial,  $N_3 = 0$ .

sphere.

When two or several topological charges  $N_a$  participate in transition, new types of Lifshitz transitions arise. Example is in Fig. 9, where two Fermi surfaces exchange their global topological charges  $N_3$ .<sup>22</sup> On both sides of the Lifshitz transition there are two Fermi surfaces, which are stabilized by their local topological charges  $N_1$ . But on the right side of transition the Fermi surfaces contain Weyl points with nonzero topological charges  $N_3 = +1$  and  $N_3 = -1$ , while on the other side of transition the Fermi surfaces are topologically trivial,  $N_3 = 0$ . At the transition line the Fermi surfaces touch each other, and their global topological charges annihilate each other.

## VI. LIFSHITZ TRANSITION AND BLACK HOLE HORIZON

Another Lifshitz transition, which involves both the Fermi surface (invariant  $N_1$ ) and the Weyl point (invariant  $N_3$ ), has relation to the black hole horizon. Let us start with the black hole. In general relativity the stationary metric, which is valid both outside and inside the black hole horizon, is provided in particular by the Painlevé-Gullstrand spacetime.<sup>23</sup> The line element of the Painlevé-Gullstrand metric is equivalent to the so-called acoustic metric:<sup>24–26</sup>

$$ds^2 = g_{\mu\nu} dx^\mu dx^\nu = -c^2 dt^2 + (d\mathbf{r} - \mathbf{v} dt)^2. \quad (5)$$

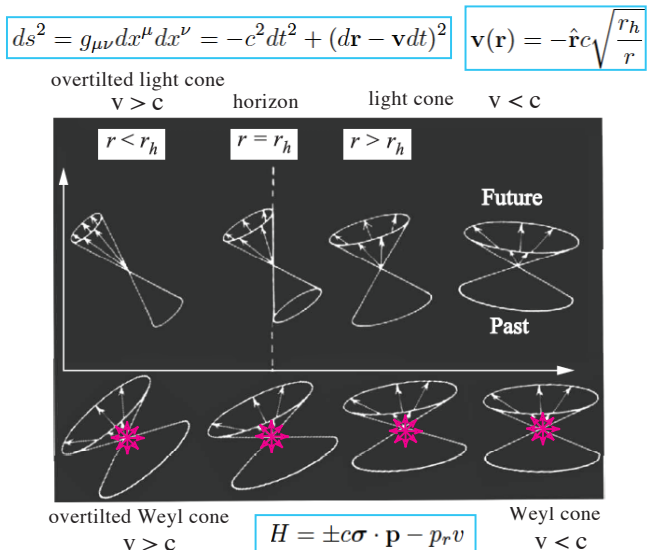


FIG. 10: Behavior of light cone (*top*) and of the corresponding Weyl cone (*bottom*) across the black hole horizon. The horizon at  $r = r_h$  serves as the surface of the Lifshitz transition between the type-I Weyl point at  $r > r_h$  and the type-II Weyl point at  $r < r_h$ . Behind the horizon the Weyl cone is overtilted and two Fermi pockets are formed, which are connected by the Weyl point, see Fig. 10 (*bottom*).

This metric is expressed in terms of the velocity field  $\mathbf{v}(\mathbf{r})$  describing the frame dragging in the gravitational field:

$$\mathbf{v}(\mathbf{r}) = -\hat{\mathbf{r}}c\sqrt{\frac{r_h}{r}}, \quad r_h = \frac{2MG}{c^2}. \quad (6)$$

Here  $M$  is the mass of the black hole;  $r_h$  is the radius of the horizon;  $G$  is the Newton gravitational constant. Behind the horizon the drag velocity exceeds the speed of light,  $|\mathbf{v}| > c$ , and particles are trapped in the hole.

The Hamiltonian of the Weyl particles in the gravitational field of the black hole described by the Painlevé-Gullstrand metric has the following form:<sup>27</sup>

$$H = \pm c\boldsymbol{\sigma} \cdot \mathbf{p} - p_r v(r), \quad v(r) = c\sqrt{\frac{r_h}{r}}. \quad (7)$$

Here the plus and minus signs correspond to the right handed and left handed Weyl fermions respectively;  $p_r$  is the radial component of the linear momentum of the particle.

The behavior of the light cone across the event horizon in the real space-time and the behavior of the corresponding Weyl cone are shown in Fig. 10. The horizon at  $r = r_h$  serves as the surface of the Lifshitz transition. When the light cone is overtilted behind the horizon in Fig. 10 (*top left*), the Weyl cone is also overtilted in such a way that the cone crosses the zero energy level, see Fig. 10 (*bottom left*). As a result two pieces of Fermi surface are formed behind the horizon. They touch each other at Weyl point in Fig. 11 (*bottom*).

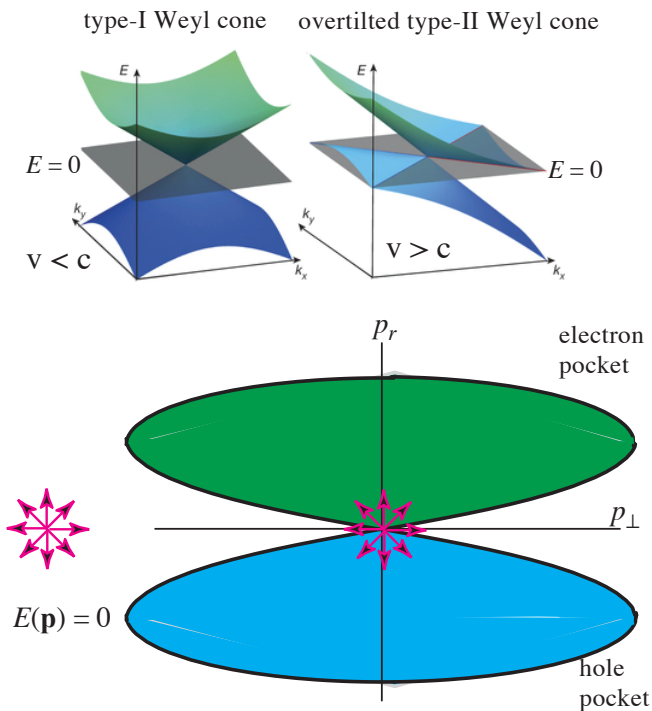


FIG. 11: Lifshitz transition between the type-I Weyl point (*top left*) and the type-II Weyl point with overtilted cone (*top right*). The type-II Weyl point connects two Fermi pockets (*bottom right*).

In the Weyl semimetals and superconductors, the Weyl point connecting two Fermi pockets is called the type-II Weyl point.<sup>28</sup> In this language the horizon represents the surface of the Lifshitz transition between the states with type-I and type-II Weyl points. This correspondence allows us to simulate the black hole using the inhomogeneous Weyl semimetal, where the transition between the type-I and type-II Weyl points takes place at some surface.<sup>29</sup> This surface would play the role of the event horizon. The formed black hole will be fully stationary in equilibrium. However, just after creation of this black hole analog, the system is not in the equilibrium state, and the relaxation process at the initial stage of equilibration looks similar to the process of the Hawking radiation.

## VII. LIFSHITZ TRANSITIONS BETWEEN GAPPED STATES VIA GAPLESS STATE

Lifshitz transitions between gapped states include transitions between the topological and non-topological insulators; transitions between the fully gapped superfluids/superconductors transitions between the 2D systems, which experience the intrinsic quantum Hall effect, etc. Here we consider such transition on example of the 2D systems, where the Hall conductance is expressed in terms of the integer-valued topological invariant  $\tilde{N}_3$  in

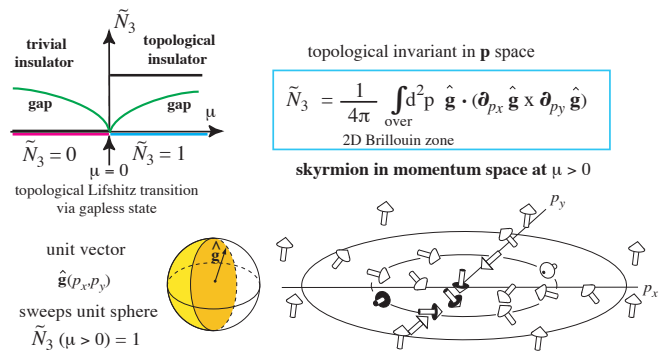


FIG. 12: Lifshitz transition between the fully gapped topologically different vacua in 2D systems, which experiences the intrinsic quantum Hall effect.<sup>30–34</sup> The Hall conductance is expressed in terms of the integer-valued topological invariant  $\tilde{N}_3$  (*top right*). The Lifshitz transition between the topological insulator with  $\tilde{N}_3 = 1$  and the trivial insulator with  $\tilde{N}_3 = 0$  takes place through the state, where the gap vanishes (*top left*).

(*Bottom*): The topologically nontrivial state with  $\tilde{N}_3 = 1$  represents the topologically nontrivial nonsingular object – skyrmion – in the 2D momentum space.

Fig. 12 (*top right*).<sup>30–33</sup> This topological invariant has the same structure as the invariant  $N_3$  in Fig. 1 (*Middle*), but the integration now is over the whole 2D Brillouin zone. This is an example of the dimensional reduction from the 3D systems with Weyl nodes to the 2D insulators.<sup>3</sup>

Fig. 12 (*top left*) demonstrates the Lifshitz transition between the topological insulator with  $\tilde{N}_3 = 1$  and the trivial insulator with  $\tilde{N}_3 = 0$ . Here the topological charge is not conserved across the Lifshitz transition, but abruptly changes recalling the first order phase transition. Nevertheless the transition occurs smoothly, because at the point of transition the gap in the energy spectrum vanishes. This can be seen on example of 2D  $p_x + ip_y$  superfluid/superconductor,<sup>34</sup> where the Lifshitz transition between the superfluid states with  $\tilde{N}_3 = 1$  and  $\tilde{N}_3 = 1$  occurs there at the same point  $\mu = 0$  as in the normal Fermi liquid. The detailed consideration shows that the Lifshitz transition represents the quantum transition of third order:<sup>35</sup> the third-order derivative  $d^3E/dg^3$  of the ground state energy  $E$  over the interaction strength  $g$  is discontinuous. Compare this with the original  $2\frac{1}{2}$  order transition,<sup>1</sup> and the  $3\frac{1}{2}$  order transition discussed recently.<sup>36</sup>

The nullification of the gap in the fermionic spectrum at the transition between the gapped vacua, suggests the scenario for the solution of the hierarchy problem: the relativistic quantum vacuum is almost massless because our Universe is very close to the line of the Lifshitz transition. The reason why nature would prefer the critical line may be that the gapless states on the transition line are able to accommodate more entropy than the gapped states.<sup>9</sup>

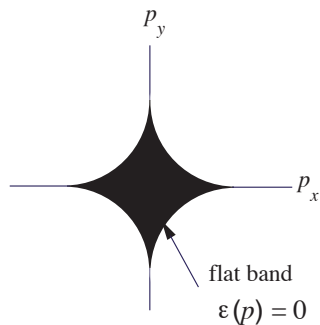


FIG. 13: Flat band emerging at the point of Lifshitz transition in Fig. 3 due to electron-electron interaction.<sup>37,38</sup> In the black region all the states have zero energy. This phenomenon of merging energy levels due to interaction is called Fermi condensation.<sup>39–41</sup>

### VIII. LIFSHITZ TRANSITIONS, FLAT BANDS AND ROOM- $T$ SUPERCONDUCTIVITY

The singularity in the density of states at the Lifshitz transition open the door for many interesting phenomena, including the formation of the flat band in the energy spectrum in Fig. 13.<sup>37,38</sup> The flat band – or the so-called Khodel-Shaginyan fermion condensate, where all the states have zero energy – is caused by electron-electron interaction.<sup>39–41</sup> This is the manifestation of the general phenomenon of merging of the energy level due to interaction. Since the flat band has huge density of electronic states, this may considerably enhance the transition temperature to superconducting state. It is possible that this effect is responsible for the occurrence of superconductivity with high  $T$  observed in the pressurized sulfur hydride:<sup>42</sup> there are some theoretical evi-

dences that the high- $T_c$  superconductivity takes place at such pressure, when the system is close to the Lifshitz transition.<sup>43,44</sup>

### IX. CONCLUSION

Topological Lifshitz transitions are ubiquitous, since they involve many types of topological structures: Fermi surfaces, Dirac lines, Dirac and Weyl points, etc. Each of these structures has their own topological invariant ( $N_1$ ,  $N_2$ ,  $N_3$ ,  $\tilde{N}_3$ , etc.), which supports the stability of a given topological structure. The topology of the shape of the Fermi surfaces and the Dirac lines, as well as the interconnection of the objects of different dimensionalities in momentum and frequency-momentum spaces, lead to numerous classes of Lifshitz transitions.

The consequences of Lifshitz transitions are important in different areas of physics. The singularities emerging at the transition are important for the construction of superconductors with enhanced transition temperature. The Lifshitz transition can be in the origin of the small masses of elementary particles in our Universe. The black hole horizon serves as the surface of Lifshitz transition between the vacua with type-I and type-II Weyl points.

### Acknowledgements

The work has been supported by the European Research Council (ERC) under the European Union’s Horizon 2020 research and innovation programme (Grant Agreement No. 694248) and by RSCF (No. 16-42-01100).

<sup>1</sup> I.M. Lifshitz, Anomalies of electron characteristics of a metal in the high pressure region, *Sov. Phys. JETP* **11**, 1130 (1960).

<sup>2</sup> P. Hořava, Stability of Fermi surfaces and  $K$ -theory, *Phys. Rev. Lett.* **95**, 016405 (2005).

<sup>3</sup> G.E. Volovik, *The Universe in a Helium Droplet*, Clarendon Press, Oxford (2003).

<sup>4</sup> G.E. Volovik, Quantum phase transitions from topology in momentum space, *Springer Lecture Notes in Physics* **718**, 31–73 (2007); cond-mat/0601372.

<sup>5</sup> G.E. Volovik, Topological Lifshitz transitions, *Fizika Nizkikh Temperatur* **43**, 57–67 (2017), arXiv:1606.08318.

<sup>6</sup> G.E. Volovik, Zeros in the fermion spectrum in superfluid systems as diabolical points, *JETP Lett.* **46**, 98–102 (1987).

<sup>7</sup> V.V. Dmitriev, A.A. Senin, A.A. Soldatov, and A.N. Yudin, Polar phase of superfluid  $^3\text{He}$  in anisotropic aerogel, *Phys. Rev. Lett.* **115**, 165304 (2015).

<sup>8</sup> C.D. Froggatt and H.B. Nielsen, *Origin of Symmetry*, World Scientific, Singapore, 1991.

<sup>9</sup> G.E. Volovik, Topological invariants for Standard Model:

from semi-metal to topological insulator, *Pis’ma ZhETF* **91**, 61–67 (2010); *JETP Lett.* **91**, 55–61 (2010); arXiv:0912.0502.

<sup>10</sup> B.G. Sidharth, A. Das, C.R. Das, L.V. Laperashvili and H.B. Nielsen, Topological Structure of the Vacuum, Cosmological Constant and Dark Energy, arXiv:1605.01169.

<sup>11</sup> Cosmological Constant and the Vacuum Stability in the Standard Model, *New Advances in Physics* **10**, 1–39 (2016).

<sup>12</sup> L.V. Laperashvili, H.B. Nielsen and C.R. Das, New results at LHC confirming the vacuum stability and Multiple Point Principle, *Int. J. Mod. Phys. A* **31**, 1650029 (2016).

<sup>13</sup> D.L. Bennett, H.B. Nielsen and C.D. Froggatt, Standard model parameters from the multiple point principle and anti-GUT, arXiv:hep-ph/9710407.

<sup>14</sup> G.E. Volovik, Coexistence of different vacua in the effective quantum field theory and multiple point principle, *JETP Lett.* **79**, 101 (2004), *Pisma ZhETF* **79**, 131 (2004), arXiv:hep-ph/0309144.

<sup>15</sup> T. Zhu, M.L. Evans, R.A. Brown, P.M. Walmsley, and A.I. Golov, Interactions between unidirectional quantized

- vortex rings, *Phys. Rev. Fluids* **1**, 044502 (2016).
- <sup>16</sup> J. von Neumann und E.P. Wigner, Über das Verhalten von Eigenwerten bei adiabatischen Prozessen, *Phys. Zeit.* **30**, 467–470 (1929).
  - <sup>17</sup> G.E. Volovik, L.P. Gor'kov, Superconductivity classes in the heavy fermion systems, *JETP* **61**, 843–854 (1985).
  - <sup>18</sup> G.E. Volovik, Dirac and Weyl fermions: from Gor'kov equations to Standard Model (in memory of Lev Petrovich Gorkov), arXiv:1701.01075.
  - <sup>19</sup> M. Creutz, Four-dimensional graphene and chiral fermions, *JHEP* 0804:017 (2008).
  - <sup>20</sup> M. Creutz, Emergent spin, *Annals Phys.* **342**, 21–30 (2014).
  - <sup>21</sup> H.B. Nielsen, M. Ninomiya: Absence of neutrinos on a lattice. I - Proof by homotopy theory, *Nucl. Phys. B* **185**, 20 (1981); Absence of neutrinos on a lattice. II - Intuitive homotopy proof, *Nucl. Phys. B* **193**, 173 (1981).
  - <sup>22</sup> F.R. Klinkhamer and G.E. Volovik, Emergent CPT violation from the splitting of Fermi points, *Int. J. Mod. Phys. A* **20**, 2795–2812 (2005); hep-th/0403037.
  - <sup>23</sup> P. Painlevé, La mécanique classique et la théorie de la relativité, *C. R. Hebd. Acad. Sci. (Paris)* **173**, 677–680 (1921); A. Gullstrand, Allgemeine Lösung des statischen Einkörperproblems in der Einsteinschen Gravitations-theorie, *Arkiv. Mat. Astron. Fys.* **16**, 1–15 (1922).
  - <sup>24</sup> W.G. Unruh, Experimental Black-Hole Evaporation, *Phys. Rev. Lett.* **46**, 1351 (1981).
  - <sup>25</sup> W.G. Unruh, Sonic analogue of black holes and the effects of high frequencies on black hole evaporation, *Phys. Rev. D* **51**, 2827–2838 (1995).
  - <sup>26</sup> P. Kraus and F. Wilczek, Some applications of a simple stationary line element for the Schwarzschild geometry, *Mod. Phys. Lett. A* **9**, 3713–3719 (1994).
  - <sup>27</sup> P. Huhtala and G.E. Volovik, Fermionic microstates within Painlevé-Gullstrand black hole, *ZhETF* **121**, 995–1003; *JETP* **94**, 853–861 (2002); gr-qc/0111055.
  - <sup>28</sup> A.A. Soluyanov, D. Gresch, Zhijun Wang, QuanSheng Wu, M. Troyer, Xi Dai, B.A. Bernevig, Type-II Weyl semimetals, *Nature* **527**, 495–498 (2015).
  - <sup>29</sup> G.E. Volovik, Black hole and Hawking radiation by type-II Weyl fermions, *JETP Lett.* **104**, 645–648 (2016), arXiv:1610.00521.
  - <sup>30</sup> H. So, Induced topological invariants by lattice fermions in odd dimensions, *Prog. Theor. Phys.* **74**, 585–593 (1985).
  - <sup>31</sup> K. Ishikawa and T. Matsuyama, Magnetic field induced multi component QED in three-dimensions and quantum Hall effect, *Z. Phys. C* **33**, 41–45 (1986).
  - <sup>32</sup> K. Ishikawa and T. Matsuyama, A microscopic theory of the quantum Hall effect, *Nucl. Phys. B* **280**, 523–548 (1987).
  - <sup>33</sup> F.D.M. Haldane, Model for a quantum Hall effect without Landau levels: Condensed-matter realization of the "Parity Anomaly", *Phys. Rev. Lett.* **61**, 2015–2018 (1988).
  - <sup>34</sup> G.E. Volovik, Analog of quantum Hall effect in superfluid  $^3\text{He}$  film, *JETP* **67**, 1804–1811 (1988).
  - <sup>35</sup> S.M.A. Rombouts, J. Dukelsky and G. Ortiz, Quantum phase diagram of the integrable  $p_x + ip_y$  fermionic superfluid, *Phys. Rev. B* **82**, 224510 (2010).
  - <sup>36</sup> G.P. Mikitik and Yu.V. Sharlai, Dirac points of electron energy spectrum, band-contact lines, and electron topological transitions of  $3\frac{1}{2}$  kind in three-dimensional metals, *Phys. Rev. B* **90**, 155122 (2014).
  - <sup>37</sup> D. Yudin, D. Hirschmeier, H. Hafermann, O. Eriksson, A.I. Lichtenstein and M.I. Katsnelson, Fermi condensation near van Hove singularities within the Hubbard model on the triangular lattice, *Phys. Rev. Lett.* **112**, 070403 (2014).
  - <sup>38</sup> G.E. Volovik, On Fermi condensate: near the saddle point and within the vortex core, *Pis'ma ZhETF* **59**, 798–802 (1994); *JETP Lett.* **59**, 830–835 (1994).
  - <sup>39</sup> V.A. Khodel and V.R. Shaginyan, Superfluidity in system with fermion condensate, *JETP Lett.* **51**, 553 (1990).
  - <sup>40</sup> G.E. Volovik, A new class of normal Fermi liquids, *JETP Lett.* **53**, 222 (1991).
  - <sup>41</sup> P. Nozieres, Properties of Fermi liquids with a finite range interaction, *J. Phys. (Fr.)* **2**, 443–458 (1992).
  - <sup>42</sup> A.P. Drozdov, M. I. Erements, I. A. Troyan, V. Ksenofontov, S. I. Shylin, Conventional superconductivity at 203 K at high pressures, *Nature* **525**, 73 (2015).
  - <sup>43</sup> Yundi Quan and Warren E. Pickett, Impact of van Hove singularities in the strongly coupled high temperature superconductor  $\text{H}_3\text{S}$ , *Phys. Rev. B* **93**, 104526 (2016).
  - <sup>44</sup> A. Bianconi and T. Jarlborg, Lifshitz transitions and zero point lattice fluctuations in sulfur hydride showing near room temperature superconductivity, *Novel Superconducting Materials* **1**, 37–49 (2015); arXiv:1507.01093.